

# Comparison of tracking methods of particle distribution in ultrafast ultrasound imaging

## 高速超音波計測における粒子分布追跡法の比較検討

Masaaki Omura<sup>1</sup>, Ryo Nagaoka<sup>1</sup>, Kunimasa Yagi<sup>1</sup>, Kenji Yoshida<sup>3</sup>, Tadashi Yamaguchi<sup>3</sup>, and Hideyuki Hasegawa<sup>1</sup> (<sup>1</sup>Univ. Toyama; <sup>2</sup>Chiba Univ.)  
大村 眞朗<sup>1</sup>, 長岡 亮<sup>1</sup>, 八木 邦公<sup>1</sup>, 吉田 憲司<sup>2</sup>, 山口 匡<sup>2</sup>, 長谷川 英之<sup>1</sup>  
(<sup>1</sup>富山大, <sup>2</sup>千葉大)

### 1. Introduction

Erythrocyte aggregation is associated with the complex cellular interactions dependent on the size and concentration of certain proteins in the plasma, intrinsic deformability of erythrocytes, their glycocalyx, and hematocrit. Although the aggregation mechanism of erythrocytes is affected by the flow conditions, the relationship between physical and flow patterns of erythrocytes must be comprehended. Our previous study has evaluated the blood flow dynamics in the numerical simulation and in-vivo measurement using the block matching method under the ultrafast plane wave transmission of the single angle<sup>1)</sup> and autocorrelation algorithm under the repeated transmission sequence of multi-angle plane waves<sup>2)</sup>.

This study develops the measurement system for ultrafast ultrasound imaging to evaluate the blood flow conditions by synchronizing other velocimetry such as high-speed camera applications with laser illumination, i.e., particle image velocimetry (PIV). Moreover, we clarify the optimum or impractical recipe of blood mimicking fluid (BMF) capable of validation of flow velocity estimation and qualifying acoustic properties such as the attenuation and backscatter coefficients.

### 2. Materials and Methods

#### 2.1 Measurement system

**Figure 1** shows the schematic diagram of the measurement system using ultrasonic and optical instrumentations. Briefly, a flow phantom was constructed by making a straight cylindrical hollow (inner diameter 6 mm, length 200 mm) in surrounding transparent medium made from 9 wt% agar (Cool Agar, Nitta Gelatin) and 91 wt% purified water. BMF that consists of white polyamide particles with 20  $\mu\text{m}$  on average (Orgasol 2002 D NAT1, Arkema) or 40  $\mu\text{m}$  (Orgasol 2002 ES4 NAT3, Arkema) diameter with transparent base solution<sup>3)</sup> was constantly flowed inside the lumen at different rotation speeds of a gear pump (2NBL10PU, Heishin) with a programmable control circuit (MR-J3-20A1, Mitsubishi).

A 7.5 MHz linear probe (UST-5412, Hitachi) and a light source (532 nm laser) with an angle unit

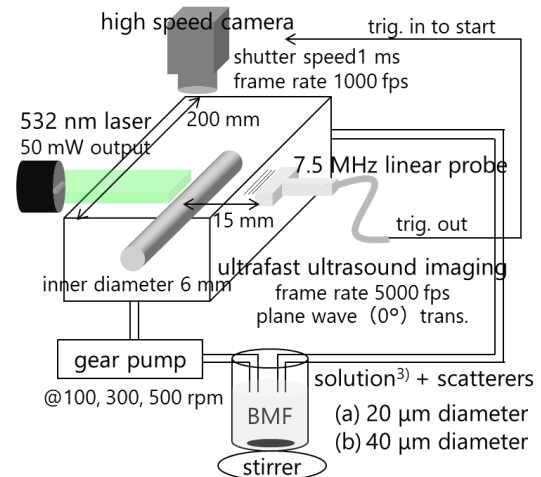


Fig. 1 Schematic diagram of measurement system. (G50, Kato Koken) coaxially arranged in the middle of the flow phantom at the maximum diameter of the lumen along the phantom long axis. A high-speed camera (k7-USB, Kato Koken) was mounted along the orthogonal axis against the planes of ultrasound scan and laser sheet. The ultrasonic and optical scattering from circulated particles in the BMF were acquired at frame rates of 5000 and 1000 fps, respectively. In the data acquisition sequence among 0.5 s, trigger signal from a research-platform scanner (RSYS0002, Microsonic) was used to synchronize collection of the optical images with acquisition of the ultrasonic radio-frequency (RF) signals.

#### 2.2 Post-processing and block matching method

Post-beamforming was carried out using the delay-and-sum method at constant f-number of 1. The beamformed RF data were sampled at axial and lateral intervals of 25  $\mu\text{m}$  and 100  $\mu\text{m}$ , respectively, where the sampling frequency and speed of sound were 31.25 MHz and 1540 m/s, respectively. The Hilbert transform was applied to compute the amplitude envelope in each receive line.

The block matching method using the normalized cross-correlation function<sup>1)</sup> was performed using amplitude envelopes of the ultrasonic RF signals and brightness of optical images. The block size was 30 $\times$ 30 pixels (0.7 $\times$ 3.0 mm<sup>2</sup> for the depth and lateral directions in the ultrasound data; 0.9 $\times$ 0.9 mm<sup>2</sup> in the optical image), and the search distance was 20 pixels. Also, the

ensemble average of the correlation function was performed for 4 ms (20 frames in the ultrasound data and 4 frames in the optical image).

### 3. Results and Discussions

**Figure 2** displays ultrasound and optical images with velocity vectors at the pump rotation speed of 500 rpm. Although speckle pattern and brightness are different due to different particle diameter and number density, the magnitude and direction of velocity vectors are consistent between ultrasound and optical images. As shown in **Fig. 3**, the parabolic profiles are confirmed in both velocities obtained by ultrasound and optical methods (temporal mean at each radial position) regardless of the different rotation speed and particle diameter. Note that the coefficient  $n$  was from 1.9 to 2.0 (laminar flow in  $n = 2.0$ ) when the following equation was fit to parabolic velocity profile  $v$  in the lumen radius  $R$  for radial distance  $r$  from the central axis.

$$v(r) = v_{\max} \left[ 1 - \left( \frac{r}{R} \right)^n \right]. \quad (1)$$

**Figure 4** compares the mean and standard deviation of velocity among the mean of velocity in each frame. The flow velocities are comparable within several cm/s (0.3-7.9% of the difference between minimum and maximum bias errors  $|v_{\text{ultrasound}} - v_{\text{optical}}| / v_{\text{optical}}$ ) except for low (0.002 wt%) or high (0.5 wt%) concentrations. The appearances of particles are considered to be too sparse or dense to track them.

Also, the green and blue shaded regions in **Fig. 4** show acceptable specifications of acoustic properties ( $\pm 3$  dB backscatter coefficient at 7.5 MHz

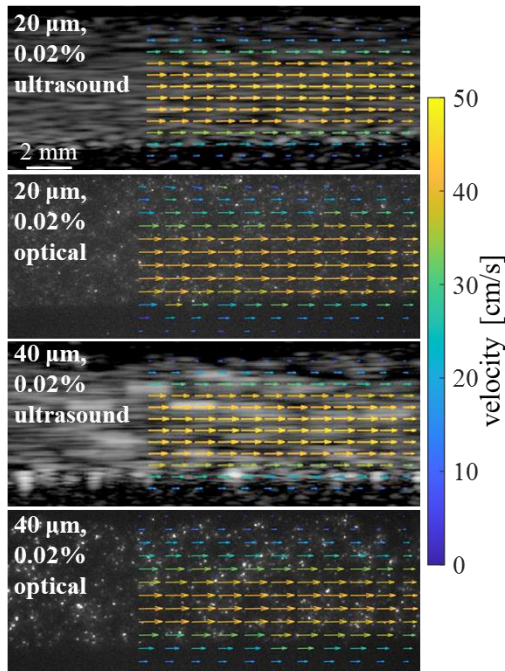


Fig. 2 Velocity vector images in ultrasound and optical data.

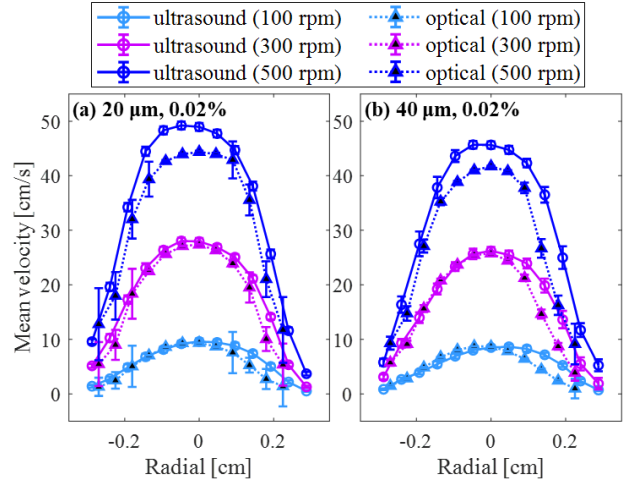


Fig. 3 Radial velocity profile of 20  $\mu\text{m}$  (a) and 40  $\mu\text{m}$  particles (b) at different rotation speeds.

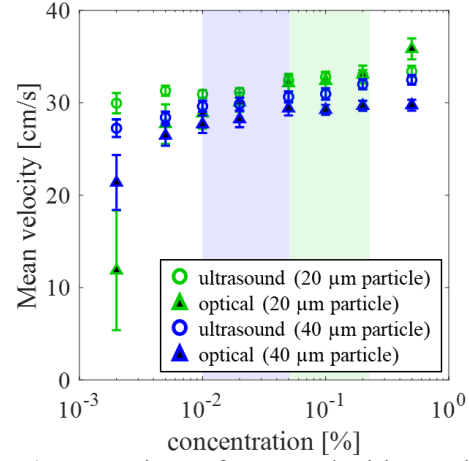


Fig. 4 Comparison of mean velocities against different concentration of two particles obtained from ultrasound and optical images.

and attenuation coefficient under 0.1 dB/cm/MHz) with reference to the BMF<sup>3</sup>). The accuracy of flow velocity estimates could be evaluated in both ultrasound and optical images within the above range.

### 4. Conclusion

This study compares ultrafast ultrasound and optical PIV methods using the block matching technique for flow velocity estimation. The difference between ultrasonically and optically estimated flow velocities were from 0.3 to 7.9% in the range of particle concentration (0.01-0.2 wt%) qualifying the acoustic properties of the BMF.

### Acknowledgment

This work was partly supported by JSPS Core-to-Core Program, and KAKENHI Grant Numbers 18KK0110, 19H04482, 20J01391.

### References

1. M. Mozumi et al.: Jpn. J. Appl. Phys., **60** (2021).
2. H. Hasegawa et al.: J. Med. Ultrason., in-press (2021).
3. K. Ramnarine et al.: Ultrasound Med. Biol., **24** (1998).